
Anatomic Validation of Spatial Normalization Methods for PET

Motoaki Sugiura, Ryuta Kawashima, Norihiro Sadato, Michio Senda, Iwao Kanno, Keiichi Oda, Kazunori Sato, Yoshiharu Yonekura and Hiroshi Fukuda

Department of Nuclear Medicine and Radiology, Institute of Development, Aging and Cancer, Tohoku University, Sendai; Aoba Brain Imaging Research Center, Telecommunications Advancement Organization, Sendai; Biomedical Imaging Research Center, Fukui Medical School, Fukui; Positron Medical Center, Tokyo Metropolitan Institute of Gerontology, Tokyo; and Department of Radiology, Research Institute for Brain and Blood Vessels, Akita, Japan

Spatial normalization methods, which are indispensable for intersubject analysis in current PET studies, have been improved in many aspects. These methods have not necessarily been evaluated as anatomic normalization methods because PET images are functional images. However, in view of the close relation between brain function and morphology, it is very intriguing how precisely normalized brains coincide with each other. In this report, the anatomic precision of spatial normalization is validated with three different methods. **Methods:** Four PET centers in Japan participated in this study. In each center, six normal subjects were recruited for both $H_2^{15}O$ -PET and high-resolution MRI studies. Variations in the location of the anterior commissure (AC) and size and contours of the brain and the courses of major sulci were measured in spatially normalized MR images for each method. Spatial normalization was performed as follows. (a) Linear: The AC-posterior commissure and midsagittal plane were identified on MRI and the size of the brain was adjusted to the Talairach space in each axis using linear parameters. (b) Human brain atlas (HBA): Atlas structures were manually adjusted to MRI to determine linear and nonlinear transformation parameters and then MRI was transformed with the inverse of these parameters. (c) Statistical parametric mapping (SPM) 95: PET images were transformed into the template PET image with linear and nonlinear parameters in a least-squares manner. Then, coregistered MR images were transformed with the same parameters used for the PET transformation. **Results:** The AC was well registered in all methods. The size of the brain normalized with SPM95 varied to a greater extent than with other approaches. Larger variance in contours was observed with the linear method. Only SPM95 showed significant superiority to the linear method when the courses of major sulci were compared. **Conclusion:** The results of this study indicate that SPM95 is as effective a spatial normalization as HBA, although it does not use anatomic images. Large variance in structures other than the AC and size of the brain in the linear method suggests the necessity of nonlinear transformations for effective spatial normalization. Operator dependency of HBA also must be considered.

Key Words: brain; PET; spatial normalization; anatomic precision; validation

J Nucl Med 1999; 40:317-322

Received Dec. 30, 1997; revision accepted May 28, 1998.

For correspondence or reprints contact: Motoaki Sugiura, MD, Department of Nuclear Medicine and Radiology, Institute of Development, Aging and Cancer, Tohoku University, 4-1 Seiryomachi Aoba-ku, Sendai 980-8575, Japan.

PET has been making an enormous contribution to studies of human brain function for the past decade (see Roland [1] for review). Intersubject analysis is essential (2) because physiological changes, such as altered regional cerebral blood flow, are usually too slight compared with noise caused by random decay of nuclide to allow statistically significant inference with a single dataset. It also aims at determining the average and common findings applicable to a group of subjects instead of describing findings for each individual subject. Spatial normalization methods developed with voxel-by-voxel analysis, which have taken the place of the region of interest (ROI) analysis, are now indispensable in current PET activation studies. The first spatial normalization method was proportional adjustment of the brain size after realignment of the brain into the three-dimensional coordinates (Talairach space) (3,4) using skull radiographs (5). Some methods have improved the precision with nonlinear as well as linear transformations at the cost of computational labor and complexity. Some have become more convenient by automation of procedures. These spatial normalization methods do not necessarily mean anatomic normalization because the PET images are not morphological images but rather are functional images. In fact, some spatial normalization methods, such as statistical parametric mapping (SPM) (6,7), even dispense with morphological images. However, it is very intriguing how precisely the spatially normalized brains anatomically coincide with each other because brain function and morphology obviously have a close relationship and the terminology used to infer brain functions are anatomic denominations based on brain atlases. In this study, we validate the anatomic precision of the spatial normalization method with linear parameters alone (linear method) (8), SPM95 (7) and human brain atlas (HBA) (9).

MATERIALS AND METHODS

Data Acquisition and Collection

Four PET centers in Japan (Tohoku, Tokyo, Akita and Fukui) participated in this study. In each center, six healthy male subjects were recruited for both $H_2^{15}O$ -PET (verb generation paradigm) (10) and high-resolution MRI studies. All subjects were strongly right-handed according to the Edinburgh Handedness Inventory with laterality quotients of >90 (11). Table 1 summarizes the

TABLE 1
Physical Characteristics and Acquisition Parameters of PET and MRI Scanners Used

	Tohoku	Tokyo	Akita	Fukui
PET				
Scanner	Headtome IV	Headtome IV	Headtome V	GE Advance
Voxel size (mm)	2 × 2 × 6.5	2 × 2 × 6.5	2 × 2 × 3.125	2 × 2 × 4.25
Number of slices	14	14	47	35
Axial FOV (mm)	91	91	150	152
Data acquisition	2D	2D	3D	3D
Counts per scan	6015	7676	26,379	16,082
MRI				
Scanner	GE Vectra	GE Sigma	Shimadzu Magnecs 50	GE Sigma Horizon
Magnetic field strength (T)	0.5	1.5	0.5	1.5
Pulse sequence	SPGR	SE	GE	SPGR
Voxel size (mm)	0.96 × 0.96 × 1.5	0.9375 × 0.9375 × 3.0	1.01 × 1.01 × 2.0	0.938 × 0.938 × 0.934

FOV = field of view; 2D = two dimensional; 3D = three dimensional; SPGR = spoiled gradient; SE = spin echo; GE = gradient echo.

Manufacturers: Headtome IV and V (Shimadzu, Kyoto, Japan); GE Advance (General Electric Medical System, France); GE Vectra, Sigma and Sigma Horizon (General Electric Medical System, Milwaukee, WI); Shimadzu Magnecs 50 (Shimadzu, Kyoto, Japan).

physical characteristics and general acquisition parameters of the PET and MRI scanners used in each center. Data analyses were performed with all 24 subjects in three PET centers (Tohoku, Tokyo and Fukui) with respective spatial normalization methods. Before spatial normalization, each subject's PET images were realigned to his MRI using the method developed by Ardekani et al. (12).

Spatial Normalization Methods

Linear Method (Tokyo). The anterior commissure (AC) and posterior commissure (PC) were determined on the sagittal planes of each subject's MR image. Then, the midsagittal plane and the border of the brain were identified on the axial and the sagittal planes. The brain size was calculated in each axis as the distance between the most distant points on the border of each hemisphere from the midsagittal plane in the x-axis, from the frontal to the occipital pole in the y-axis and from AC-PC to the vertex of the brain in the z-axis. Then each MR image was proportionally adjusted to the Talairach space (3) with a different scaling factor for each axis (8).

HBA (Tohoku). Atlas structures (contours of the brain, ventricles and central, lateral and occipitoparietal sulci in both hemispheres) of the standard brain were adjusted manually to the MR image of each subject using four linear and four nonlinear transformation parameter sets, including local transformation parameters. Manual adjustment procedures were performed by the first author for all subjects. Each MR image was transformed into the standard brain anatomy using the inverse of these parameters (9).

SPM95 (Fukui). Each sample PET image was automatically transformed with the SPM95, which uses 12 linear and 6 quadratic parameters to minimize the sum of squares between the sample PET image and template PET image (7). Thereafter, each MR image was transformed with the same parameters used in transformation of the same subject's PET image.

Evaluation Method

Evaluation of the anatomic precision in spatial normalization was performed as follows. First of all, 72 spatially normalized MR images (three methods × 24 subjects) were registered in a Sun SPARC (Sun Microsystems, Palo Alto, CA) workstation and shown with the help of Analyze (Biomedical Imaging Resource; Mayo Foundation, Rochester, MN) or HBA (9). The location of the AC,

the size and contours of the brain and the courses of five major sulci (central sulci, lateral sulci, calcarine sulci, occipitoparietal sulci and cingulate sulci bilaterally) were then measured in spatially normalized MR images for each method as described later.

Locations of the AC were determined visually with reference to its posterior margin. Mean location was calculated as the center of gravity of the AC location for the 24 brains. Deviation was calculated as the distance from the mean location.

The brain size, which means the length in the anterior-posterior direction and the width, was determined by measuring four points (anterior, posterior, right and left) on the AC-PC plane. The values of y coordinates at the frontal and occipital poles and x coordinates at the most distant points on the border of each hemisphere from the midsagittal plane were measured. Deviations were calculated as differences from the mean values in each direction.

The contours and major sulci were shown as line drawings consisting of 1 × 1 × 1-mm voxels. The contours were shown on the AC-PC plane (horizontal), a projected contour of sagittal planes (sagittal) and a vertical plane passing through the PC (coronal). The courses of the central and lateral sulci on the brain surface were shown for transaxial and coronal planes, respectively, and the calcarine, occipitotemporal and cingulate sulci on the medial surfaces of the brains were shown on the parasagittal plane, 8 mm away from the midsagittal plane for each hemisphere. The deep courses of the central sulci within the brains were shown for the transaxial plane at both 35 and 50 mm above the AC-PC plane. All

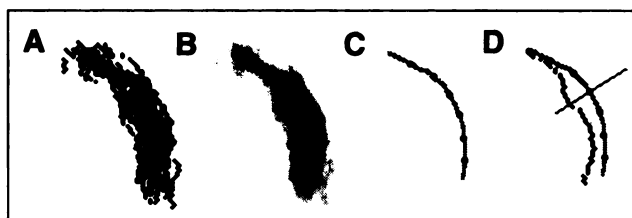


FIGURE 1. Evaluation methods for brain contours and courses of sulci. Courses of right central sulci are shown as examples. (A) Twenty-four line drawings; (B) mean course manually drawn from blurred line drawings; (C) measuring points with 10-mm distance from each other; and (D) deviation measured on line perpendicular to mean course at measuring point.

TABLE 2
Variation in Location of Anterior Commissure (AC)
and Size of Normalized Brain

	Linear (mm)	HBA (mm)	SPM95 (mm)	
AC	2.23 ± 1.03	2.17 ± 1.05	2.33 ± 0.94	
Size				
Anterior	1.10 ± 0.62	1.49 ± 1.09	2.33 ± 1.92	SPM > linear SPM > linear and HBA
Posterior	1.40 ± 1.24	1.25 ± 1.05	2.83 ± 2.47	
Right	0.78 ± 0.69	1.14 ± 0.90	0.77 ± 0.44	
Left	1.30 ± 0.67	0.96 ± 0.51	1.73 ± 1.08	SPM > HBA

HBA = human brain atlas; SPM = statistical parametric mapping.
Mean ± SD for variation in anterior commissure (AC) location and size for 24 normalized brains. The right-hand column indicates significant differences between methods ($P < 0.05$ with analysis of variance and two-sample *t* tests with Welch's correction).

24 drawings for each structure were placed on the identical stereotactic space (Fig. 1A) for each method. The mean contours and courses of sulci were shown manually on projected images of blurred line drawings on the representative plane (Fig. 1B). Measuring points on the mean contour and courses of sulci were determined. The interval of points was 10 mm for each structure (Fig. 1C). The deviations from the mean contour and courses of sulci were measured for each representative plane at every measuring point on the line perpendicular to the mean structure (Fig. 1D). The value representing the deviation of each contour or major sulci of each subject was calculated as the root mean square of the deviation at all measuring points. The precision of the anatomic normalization was evaluated with mean values for root mean square of all subjects for each structure. The precision was then compared among three methods in each structure with the analysis of variance and two-sample *t* test using Welch's correction post hoc.

TABLE 3
Variation in Contours of Normalized Brain

	Linear (mm)	HBA (mm)	SPM95 (mm)	
Horizontal	1.84 ± 0.59	1.35 ± 0.30	1.52 ± 0.67	Linear > HBA
Sagittal	2.68 ± 0.79	2.19 ± 0.61	2.58 ± 1.04	
Coronal	2.23 ± 0.89	2.15 ± 0.56	1.95 ± 0.58	

HBA = human brain atlas; SPM = statistical parametric mapping.
Mean ± SD for variation in the contours of 24 normalized brains, calculated as root mean square of deviation from mean contours at all measuring points. The right-hand column indicates significant differences between methods ($P < 0.05$ with analysis of variance and two-sample *t* tests with Welch's correction).

RESULTS

Data for the variation in the location of the AC and the size of the normalized brain with each method are summarized in Table 2. No significant differences were found for the AC. The sizes of the brains normalized with the SPM95 had significantly ($P < 0.05$ for each comparison) larger variation for the anterior, posterior and left sides compared with those normalized with the other two methods.

Contours of the 24 brains normalized with each method are shown in Figure 2. Relatively large variation was seen in the linear method. Cases with large deviation in the temporal lobe with the linear method and in the frontal lobe and occipital lobe with the SPM95 were observed. It was shown that in some brains with SPM95, the most inferior part of the temporal lobe is out of the conventional SPM95 frame. Quantitation of variation was performed separately for the horizontal, sagittal and coronal planes (Table 3). The vertex in the sagittal and coronal planes and the temporal base in

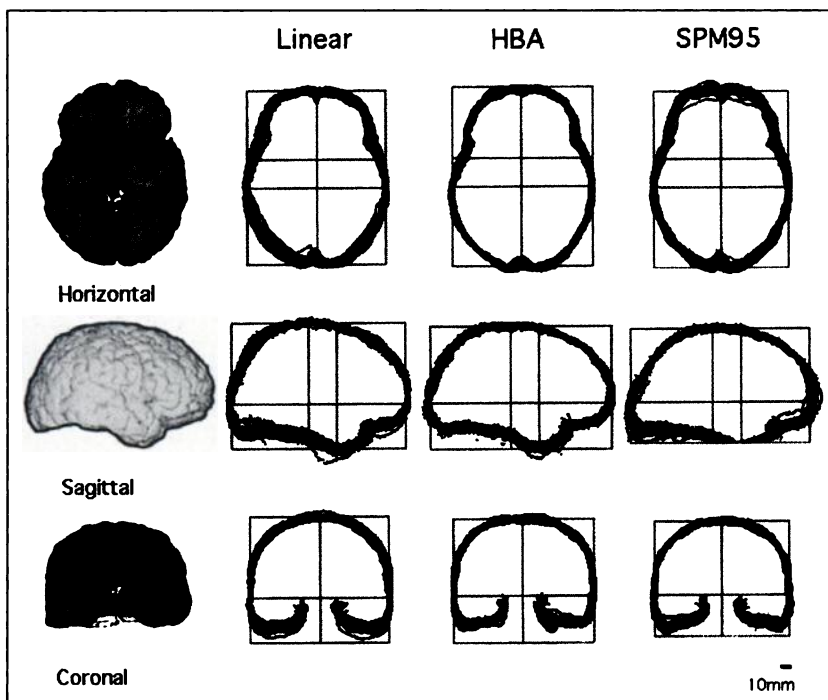


FIGURE 2. Contours of normalized brain. Line drawings are superimposed on Talairach frame. Standard HBA brain in corresponding plane or projected image is shown on left.

the sagittal plane were not evaluated because of missing data. Significantly larger variation with the linear method compared with the HBA was noted for the contours in the horizontal plane.

The courses of the sulci on lateral and medial surfaces of the brains normalized with each method and projected onto sagittal planes are shown in Figure 3. Quantitative analysis (Table 4) showed significantly large variations in the central and calcarine sulci in the right hemisphere with the linear method compared with the SPM95 case. The courses of the central sulci within the brain normalized with each method also varied at both transaxial levels (Fig. 4). The right central sulci of the brains normalized with the linear method had larger variations than those normalized with SPM95 (Table 4).

The case that had a large deviation in the contour of the frontal lobe by SPM95 normalization showed exceptionally high radioactivity in the nasal cavity and maxillary sinus.

DISCUSSION

To our knowledge, this is the first trial of an anatomic evaluation of spatial normalization by SPM95. The results showed precise anatomic normalization of the courses of the

major sulci with SPM95. There was high effectiveness in the spatial normalization procedure with SPM95, without the use of anatomic images or even a priori reference to brain position. This suggests a general coincidence between brain function and morphology and confirms the validity of the least-squares approach.

For interpretation of the results, particular attention must be paid to measurement errors. Although adjustment of the AC location and brain size is made with the linear method, the mean variation exceeded 2 and 1 mm, respectively, for these parameters in three directions. Variation may thus include a measurement factor, but it is reasonable to assume that errors may distribute normally, at least in the same evaluation procedure, and may be compensated by statistical analysis.

In the brains normalized with the linear method, the variation of the AC location and brain size were comparable to those with the HBA and were smaller than those with the SPM95, but the contours and the courses of the major sulci varied more. The results show the necessity for nonlinear parameters for effective spatial normalization. Spatial normalization for intersubject analysis in PET activation studies is

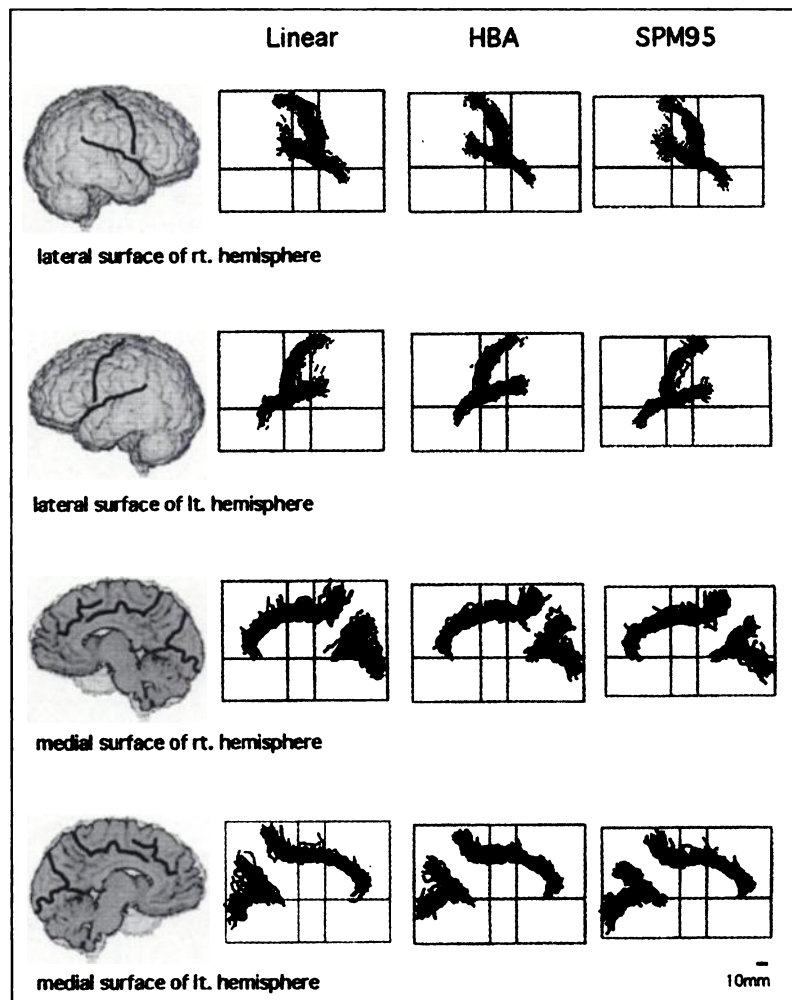


FIGURE 3. Courses of major sulci (surface). Line drawings are superimposed on Talairach frames. Standard HBA brain in corresponding view is shown on left. SPM = statistical parametric mapping; rt. = right; lt. = left.

TABLE 4
Variation in Courses of Major Sulci
of Normalized Brain

	Linear (mm)	HBA (mm)	SPM95 (mm)	
Right lateral surface				
Central sulcus	4.27 ± 2.30	3.93 ± 1.53	3.12 ± 1.32	
Lateral sulcus	3.31 ± 1.68	2.78 ± 1.08	3.08 ± 1.21	
Left lateral surface				
Central sulcus	3.87 ± 1.71	4.11 ± 1.80	3.99 ± 1.46	
Lateral sulcus	3.20 ± 1.69	3.17 ± 1.40	2.50 ± 1.14	
Right medial surface				
Calcarine sulcus	5.74 ± 2.93	4.66 ± 1.54	4.08 ± 1.91	Linear > SPM
Occipitoparietal sulcus	3.85 ± 2.24	3.49 ± 1.91	3.41 ± 1.34	
Cingulate sulcus	4.50 ± 1.58	4.33 ± 1.65	4.20 ± 1.46	
Left medial surface				
Calcarine sulcus	4.19 ± 1.99	3.77 ± 1.80	3.80 ± 1.65	
Occipitoparietal sulcus	4.31 ± 2.33	3.61 ± 1.75	3.57 ± 1.68	
Cingulate sulcus	4.15 ± 1.56	4.04 ± 1.14	3.74 ± 1.23	
Deep structure of right central sulci				
35 mm above AC-PC plane	4.00 ± 3.01	3.09 ± 1.23	2.60 ± 1.24	
50 mm above AC-PC plane	3.98 ± 2.81	3.07 ± 1.30	2.49 ± 1.13	Linear > SPM
Deep structure of left central sulci				
35 mm above AC-PC plane	2.92 ± 1.82	2.86 ± 1.38	2.76 ± 2.16	
50 mm above AC-PC plane	3.96 ± 2.24	3.06 ± 1.57	3.02 ± 1.30	

HBA = human brain atlas; SPM = statistical parametric mapping; AC-PC = anterior commissure-posterior commissure.

Mean ± SD for variation in the courses of major sulci in 24 normalized brains, calculated as root mean square of deviation from mean courses at all measuring points. The right-hand column indicates significant differences between methods ($P < 0.05$ with analysis of variance and the two-sample t tests with Welch's correction).

not expected to make subjects' brains conform completely to the same shape. Residual anatomic variation must then be overcome by smoothing, usually with a Gaussian kernel. Inaccurate spatial normalization results in a decrease in

detecting power. Based on the concept of local-maximum sampling (2) and the "average brain" (13), which assumes that spatial averaging decreases anatomic variation, activation sites can be detected with precision above image resolution, but this concept may not necessarily work as expected with the number of subjects for which PET activation studies are usually performed. Therefore, inaccurate spatial normalization results in a decrease of reliability about the location of the activated site.

Although SPM95 was found in this study to spatially normalize brains in a valid fashion in general, some cases with large deviation, one of which was possibly caused by radioactivity in the nasal mucous and maxillary cavity, were encountered. Careful elimination of such ill-normalized cases is clearly necessary. It is preferable to confirm the normalization with morphological images that have been normalized using the same parameters as applied to PET images, especially when the number of subjects is small. Provided that there is awareness of the possibility of failure in normalization and of limitations in the reliability of anatomic inference, spatial normalization with SPM95 may be sufficiently practical for PET studies. Where failure in spatial normalization with SPM95 is apparent, this would indicate an abnormal distribution of radioactivity and would trigger a study of individual variation. It might therefore open the way to new insights into the relation between the normal brain function and morphology.

In this study, HBA was found to adjust the contours and the size of the brain well, but this method was intermediate between the linear method and SPM95 in terms of the courses of major sulci. Anatomic variation for structures of the brain normalized with HBA was evaluated previously (9). Although it is difficult to compare the results because of differences in evaluation methods, a tendency for varied contours and more accurate sulci adjustment was noted. This may reflect operator dependency on the spatial normalization with HBA. In addition, HBA requires detailed neuroanatomic knowledge and is very labor intensive. Nevertheless, such direct manipulation of morphological images prevents accidental failure of spatial normalization and allows reliable inferences to be made about function and anatomy. It is therefore suitable for PET activation studies with small numbers of subjects.

Recently, in response to the demands of the study in anatomic variation of the human brain, which aims at making standard brain as a probability map of macroscopic, cytoarchitectural, immunochemical and functional anatomy (14,15), many new spatial normalization methods that use nonlinear warping with extraordinary flexibility have been proposed (16,17). Although there are problems, such as perturbation of statistical assumption by excess local transformation and a tremendous demand of computational support, it can be expected that application of these new methods will herald a new stage in PET studies.

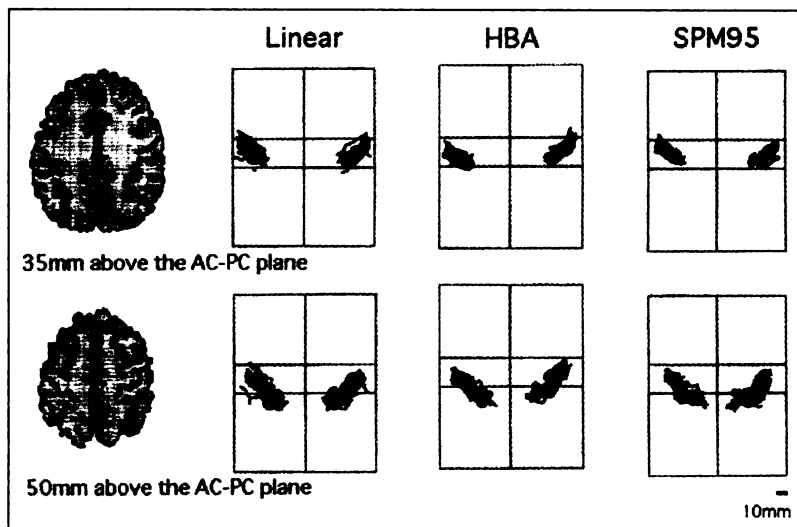


FIGURE 4. Courses of central sulci within brain. Line drawings are superimposed on Talairach frames. Standard HBA brain in corresponding plane is shown on left. SPM = statistical parametric mapping; AC-PC = anterior commissure-posterior commissure.

ACKNOWLEDGMENTS

This work was performed as one of the common-use programs of Nishina Memorial Cyclotron Center, Japan Radioisotope Association. This work was supported by grant 97L00202 from the JSPS-RFTF, by grants in aid for scientific research on priority research from the Japanese Ministry of Education, Science, Sports and Culture (10164206, 0927102) and by the Telecommunications Advancement Organization of Japan.

REFERENCES

1. Roland PE. *Brain Activation*. New York, NY: Wiley & Sons; 1993.
2. Fox PT, Mintun MA, Reiman EM, Raichle ME. Enhanced detection of focal brain responses using intersubject averaging and change-distribution analysis of subtracted PET images. *J Cereb Blood Flow Metab*. 1988;8:642-653.
3. Talairach J, Zilka G, Tournoux P, et al. *Atlas d'Anatomie Stereotaxique du Telencephale*. Paris, France: Masson; 1967.
4. Talairach J, Tournoux P. *Co-planar Stereotaxic Atlas of the Human Brain*. New York, NY: Thieme; 1988.
5. Fox PT, Perlmutter JS, Raichle ME. A stereotactic method of anatomical localization for positron emission tomography. *J Comput Assist Tomogr*. 1985;9:141-153.
6. Friston KJ, Frith CD, Liddle PF, Frackowiak RSJ. Plastic transformation of PET images. *J Comput Assist Tomogr*. 1991;15:634-639.
7. Friston KJ, Ashburner J, Frith CD, Poline J-B, Heather JD, Frackowiak RSJ. Spatial registration and normalization of images. *Hum Brain Mapping*. 1995;2:165-189.
8. Senda M, Kanno I, Yonekura Y, et al. Comparison of anatomical standardization methods regarding the sensorimotor foci localization and between-subject variation in $H^2_{15}O$ PET activation, a three-center collaboration study. *Ann Nucl Med*. 1994;8:201-207.
9. Roland PE, Grafelds CJ, Wahlin J, et al. Human brain atlas: for high-resolution functional and anatomical mapping. *Hum Brain Mapping*. 1994;1:173-184.
10. Poline JB, Vandenberghe R, Holmes AP, Friston KJ, Frackowiak RSJ. Reproducibility of PET activation studies: lessons from a multi-center European experiment EU concerted action of functional imaging. *Neuroimage*. 1996;4:34-54.
11. Oldfield RC. The assessment and analysis of handedness: the Edinburgh inventory. *Neuropsychologia*. 1971;9:97-113.
12. Ardekani BA, Braun M, Hutton BF, Kanno I, Iida H. A fully automatic multimodality image registration algorithm. *J Comput Assist Tomogr*. 1995;19:615-623.
13. Woods RP. Correlation of brain structure and function. In: Toga AW, Mazziotta JC, eds. *Brain Mapping—The Methods*. London, England: Academic Press; 1995:313-342.
14. Roland PE, Zilles K. Brain atlas—a new research tool. *Trends Neurosci*. 1994;17:458-467.
15. Mazziotta JC, Toga AW, Evans AC, Fox PT, Lancaster JL. Digital brain atlases [letter and reply]. *Trends Neurosci*. 1995;18:210-211.
16. Collins DL, Holmes CJ, Peters TM, Evans AC. Automatic 3-D model-based neuroanatomical segmentation. *Hum Brain Mapping*. 1995;3:190-208.
17. Schormann T, Henn S, Zilles K. A new approach to fast elastic alignment with applications to human brain. *Lecture Notes Computer Sci*. 1996;1131:337-342.